



Cytofluorometric assessment of calreticulin exposure on CD38⁺ plasma cells from the human bone marrow

Manuel Beltrán-Visiedo^a, Alfonso Serrano-Del Valle^b,
Nelia Jiménez-Aldúan^b, Ruth Soler-Agesta^{a,b}, Javier Naval^b,
Lorenzo Galluzzi^{a,c,d,*}, and Isabel Marzo^{b,*}†

^aDepartment of Radiation Oncology, Weill Cornell Medical College, New York, NY, United States

^bApoptosis, Immunity & Cancer Group, IIS Aragón, University of Zaragoza, Zaragoza, Spain

^cSandra and Edward Meyer Cancer Center, New York, NY, United States

^dCaryl and Israel Englander Institute for Precision Medicine, New York, NY, United States

*Corresponding authors: e-mail address: deado80@gmail.com; imarzo@unizar.es

Contents

1. Introduction	190
2. Materials	193
2.1 Common disposables	193
2.2 Cells and reagents	193
2.3 Equipment	193
2.4 Software	194
3. Methods	194
3.1 Culture and isolation of mononuclear cells from human BM samples	194
3.2 Surface-expose CALR quantification	195
3.3 Acquisition and gating	195
3.4 Surface-exposed PS quantification	196
3.5 Acquisition and gating	197
4. Notes	197
5. Concluding remarks	199
Acknowledgments	200
Conflicts of interests	201
References	201

† Co-senior authors.

Abstract

Exposure of the endoplasmic reticulum chaperone calreticulin (CALR) on the surface of stressed and dying cells is paramount for their effective engulfment by professional antigen-presenting cells such as dendritic cells (DCs). Importantly, this is required (but not sufficient) for DCs to initiate an adaptive immune response that culminates with an effector phase as well as with the establishment of immunological memory. Conversely, the early exposure of phosphatidylserine (PS) on the outer layer of the plasma membrane is generally associated with the rapid engulfment of stressed and dying cells by tolerogenic macrophages. Supporting the clinical relevance of the CALR exposure pathway, the spontaneous or therapy-driven translocation of CALR to the surface of malignant cells, as well as intracellular biomarkers thereof, have been associated with improved disease outcome in patients affected by a variety of neoplasms, with the notable exception of multiple myeloma (MM). Here, we describe an optimized protocol for the flow cytometry-assisted quantification of surface-exposed CALR and PS on CD38⁺ plasma cells from the bone marrow of patients with MM. With some variations, we expect this method to be straightforwardly adaptable to the detection of CALR and PS on the surface of cancer cells isolated from patients with neoplasms other than MM.



1. Introduction

Most often, mammalian cells die in an immunologically silent or even tolerogenic manner, especially (1) when cell death is part of a purely physiological program of development or adult tissue homeostasis (Fuchs & Steller, 2015), and (2) when cell death is unrelated to bacterial or viral infection (Kroemer et al., 2022). From an organismal perspective, this is particularly important to avoid unwarranted autoreactive/autoimmune conditions that may otherwise emerge from physiological tissue turnover or from pathological conditions that cause cell death in the absence of infection (*e.g.*, ischemia, trauma) (Kroemer et al., 2022). In line with this notion, several mechanisms are in place to ensure that infection-unrelated cell death in mammals, which most often is precipitated by the apoptotic machinery (Czabotar & Garcia-Saez, 2023; Diepstraten et al., 2022; Vitale et al., 2023), goes unnoticed by the immune system. For instance, apoptotic caspases such as caspase 3 (CASP3) proficiently shut down inflammatory reactions as potentially elicited by mitochondrial outer membrane permeabilization (MOMP) and the consequent release of interferogenic mitochondrial DNA (mtDNA) in the cytosol (Giampazolias et al., 2017; Han et al., 2020; Ning et al., 2019; Rodriguez-Ruiz et al., 2019; Rongvaux et al., 2014; White et al., 2014; Yamazaki et al., 2020). Moreover CASP3 effectively stimulates the secretion

of immunosuppressive molecules such as prostaglandin E₂ (PGE₂) (Böttcher et al., 2018; Huang et al., 2011; Zelenay et al., 2015), as well as the exposure of phosphatidylserine (PS) on the outer leaflet of the plasma membrane, which elicits the rapid and immunologically silent clearance of dying cells by macrophages (Boada-Romero et al., 2020; Doran et al., 2020; Fadok et al., 1992; Mehrotra & Ravichandran, 2022; Rothlin et al., 2021). Reflecting the critical importance of an efficient and immunologically silent removal of dying cells and their corpses by macrophages, *Jmjd6*^{-/-} mice (which lack the receptor for surface-exposed PS) die at birth owing to the accumulation of dead cells in the brain and lung (Fadok et al., 2000; Li et al., 2003).

In pathological settings, the death of mammalian cells can also promote inflammation potentially coupled with adaptive immune reactions (Galluzzi et al., 2023). Most often, cell death drives inflammation in the absence of adaptive immunity when (1) cell death is not caused by infectious agents, and (2) the amount of dying cells, which release a number of adjuvant-like molecules cumulatively known as damage-associated molecular patterns (DAMPs) overwhelms the phagocytic capacity of macrophages (Galluzzi et al., 2020a). Conversely, adaptive immune responses culminating with a cytotoxic T lymphocyte (CTL)-mediated effector phase and the establishment of immunological memory can be initiated by dying cells when (1) they express endogenous antigenic determinants that are not covered by central tolerance (antigenicity), (2) cell death is associated with the spatiotemporally coordinated release of key DAMPs and cytokines that recruit and license professional antigen-presenting cells (APCs) such as dendritic cells (DCs) (adjuvanticity), and (3) the microenvironment of dying cells allows for the recruitment of DC precursors, their activation and their migration to secondary or tertiary lymphoid organs for antigen presentation to CD4⁺ and CD8⁺ T cells (microenvironmental permissiveness) (Galluzzi et al., 2020a; Gong et al., 2020; Kroemer et al., 2022; Krysko et al., 2012; Matzinger, 2002; Mellman et al., 2023). Interestingly, such an immunogenic form of cell death is not only driven by pathogens, but also by a variety of chemical and physical stimuli, provided that the antigenicity criteria is met (Jhunjhunwala et al., 2021; Lang et al., 2022; Stern et al., 2024). These include (but not limited to): specific chemotherapeutics (Galluzzi et al., 2020b; Sprooten et al., 2023), radiation therapy (Cytlak et al., 2022; McLaughlin et al., 2020; Rodriguez-Ruiz et al., 2020), oncolytic agents (Harrington et al., 2019; Kepp et al., 2020; Palanivelu et al., 2022; Shalhout et al., 2023), photodynamic therapy (Adkins et al., 2014; Garg et al., 2016), and extracorporeal photopheresis (Tatsuno et al., 2019;

Ventura et al., 2018). Interestingly, while apoptotic caspases have been shown to limit the immunogenicity of cell death by a number of mechanisms, both apoptotic and non-apoptotic instances of immunogenic cell death (ICD) have been reported (Casares et al., 2005; Efimova et al., 2020; Hadian & Stockwell, 2023; Lei et al., 2022; Yatim et al., 2015; Yuan & Ofengeim, 2023).

Calreticulin (CALR) is an endoplasmic reticulum (ER) chaperone that exerts prominent roles in protein folding, Ca^{2+} homeostasis and MHC Class I antigen presentation (Fucikova et al., 2021). Importantly, stressed and dying cells can expose CALR on their surface (Obeid et al., 2007), where it delivers potent pro-phagocytic signals to a variety of myeloid cells (including DC precursors) that express low-density lipoprotein receptor-related protein 1 (LRP1, also known as CD91) and possibly other scavenger receptors (Gardai et al., 2005; Ogden et al., 2001; Pawaria & Binder, 2011; Vandivier et al., 2002). Mechanistically, the ICD-associated CALR exposure is elicited in the context of the so-called “integrated stress response” (ISR), which is demarcated by the inactivating prokaryotic translation initiation factor 2 subunit alpha (EIF2S1, best known as eIF2 α) (Bezu et al., 2018a, 2018b; Panaretakis et al., 2009).

Supporting the clinical relevance of this pathways in oncological settings, the level of surface-exposed CALR (as well as the degree of eIF2 α phosphorylation) has been associated with improved clinical outcome in several cohorts of patients with cancer (Fucikova et al., 2015). Specifically, the spontaneous or therapy-driven exposure of CALR on the cancer cell surface has been linked with superior disease outcome in cohorts of patients with non-small cell lung carcinoma (NSCLC) (Fucikova et al., 2016a), acute myeloid leukemia (AML) (Fucikova et al., 2016b; Truxova et al., 2020; Wemeau et al., 2010), neuroblastoma (Hsu et al., 2005), colorectal carcinoma (Peng et al., 2010), as well as endometrial and ovarian cancer (Kasikova et al., 2019; Xu et al., 2018). That said, elevated levels of surface-exposed CALR have also been associated with poor clinical outcome in patients with multiple myeloma (MM) (Serrano Del Valle et al., 2022).

Here, we provide a simple cytofluorometric protocol to quantify CALR and PS exposure on the membrane of CD38⁺ plasma cells isolated the bone marrow (BM) of patients with MM. With some variations, this method should be straightforwardly adaptable to the assessment of surface-exposed CALR and PS on malignant cells from patients with a variety of tumors.



2. Materials

2.1 Common disposables (see Note 1)

- Acrodisc[®] Syringe Filters for Prefiltration, 0.22 μ M (Cytiva, #17194361)
- Falcon[™] 5 mL Round-Bottom Polypropylene Test Tubes Without Cap (Fisher Scientific, #10519901)
- Nunc[™] 15 mL Conical Sterile Polypropylene Centrifuge Tubes (Thermo Scientific[™], #339650)
- Nunc[™] 50 mL Conical Sterile Polypropylene Centrifuge Tubes (Thermo Scientific[™], #339652)

2.2 Cells and reagents (see Note 1)

- 7-Actinomycin D (7-AAD) Viability Staining Solution (Biolegend, #420403)
- Annexin V-DY-634 PI Apoptosis Staining/Detection Kit (abcam, #ab214484) (see Note 2)
- BD Pharmingen[™] APC Mouse Anti-Human CD38 (HIT2) (BD Pharmingen[™], #560980)
- BD Pharmingen[™] FITC Mouse Anti-Human CD38 (HIT2) (BD Pharmingen[™], #560982)
- Bone marrow (BM) samples from patients with MM or other plasma cell malignancies (see Notes 3–4)
- Calreticulin monoclonal antibody (FMC 75), DyLight[™] 488 (Enzo Life Sciences, #ADI-SPA-601-488-F)
- Fetal bovine serum (FBS), Sigma-Aldrich, #F7524)
- Gibco[™] RPMI 1640 Medium, GlutaMAX[™] Supplement (Gibco, #12027599)
- Histopaque[®]-1077 (Sigma-Aldrich, #10771)
- Mouse IgG1 Isotype Control (MOPC-21), DyLight[™] 488 (Invitrogen, #MA1-191-D488)
- PBS—Phosphate-Buffered Saline (10 \times) pH 7.4, RNase-free (Thermo Scientific[™], #AM9624) (see Note 5)
- Trypan Blue solution (Sigma-Aldrich, #T8154)

2.3 Equipment (see Note 1)

- Benchtop cell counter, such as Countess II automated cell counter (Invitrogen) (see Note 6)

- Benchtop centrifuge, such as Allegra[®] X-15R Centrifuge (Beckman Coulter)
- Class II vertical laminar air flow cabinet, such as Bio II Advance Plus (Telstar)
- Flow cytometer equipped with lasers for acquisition of fluorescence from FITC and DyLight[™] 488 (488nm, 610/20nm filter), 7-AAD (488nm, 690/50 filter) and DY-634 (640nm, 710/50nm filter), such as BD FACSCalibur[™] (BD Biosciences)
- Humidified cell culture incubator, such as Heraeus Heracell 150i (Thermo Scientific[™]) (*see Note 7*)

2.4 Software (*see Note 1*)

- FlowJo[™] v. 7.6.1 (FlowJo LLC)
- Prism v. 10.0.1 (GraphPad)



3. Methods

3.1 Culture and isolation of mononuclear cells from human BM samples

3.1.1 Medium preparation

1. Heat FBS at 56 °C for 30min in a water bath, and centrifuge at 560 × *g* for 15 min (*see Note 8*).
2. Filter supernatant with a sterile 0.22 μm syringe filter and collect in a sterile 50 mL conical tube.
3. Generate complete bone marrow mononuclear cell (BMMC) medium by complementing RPMI 1640 Medium, GlutaMAX[™] Supplement with 10% (v:v) heat-inactivated FBS.

3.1.2 BMMC isolation

1. Add 3–4 mL Histopaque[®]-1077 (according to the volume of BM sample) (*see Note 9*) to sterile 15 mL conical tubes.
2. Dilute BM samples 1:2 (v:v) with RPMI 1640 Medium, GlutaMAX[™] Supplement (without heat-inactivated FBS) or PBS.
3. Gently layer BM samples onto Histopaque[®]-1077 by ensuring that phases remain separated (*see Notes 10, 11*).
4. Centrifuge at 500 × *g* for 20min while deactivating the rotor brake (*see Note 12*).
5. Remove the upper plasma layer with a P1000 micropipette or a sterile Pasteur pipette (*see Note 13*).

6. Collect BMBCs (which are located at the interphase between the plasma and Histopaque[®]-1077 phase) with a P1000 micropipette and transfer them into a sterile 15 mL conical tube containing 10 mL RPMI 1640 Medium, GlutaMAX[™] Supplement.
7. Thoroughly wash BMBCs twice with RPMI 1640 Medium, GlutaMAX[™] Supplement to eliminate traces of Histopaque[®]-1077 by centrifuging at $335 \times g$ for 5 min and discarding the supernatant at each washing cycle.
8. Resuspend BMBCs in 10 mL BMBC complete medium.
9. Determine BMBC density by mixing 30 μ L Trypan Blue solution and 30 μ L BMBC suspension and counting with the Countess II automated cell counter (*see Note 6*).

3.2 Surface-expose CALR quantification

1. Transfer 5×10^5 primary BMBCs to 5 mL Round-Bottom Polypropylene Test Tubes (*see Note 14*), and centrifuge at $335 \times g$ for 5 min.
2. Resuspend BMBCs in 100 μ L PBS complemented with 5% FBS plus 2 μ L Calreticulin monoclonal antibody (FMC 75), DyLight[™] 488 or Mouse IgG1 Isotype Control (MOPC-21), DyLight[™] 488, 8 μ L APC Mouse Anti-Human CD38 (HIT2), and 1 μ L 7-AAD Viability Staining Solution.
3. Incubate at 4 °C for 30 min in the darkness (*see Note 15*).
4. Centrifuge BMBCs at $335 \times g$ for 5 min and resuspend them in 200–300 μ L PBS for acquisition of fluorescent signals by flow cytometry.

3.3 Acquisition and gating

1. Flow cytometry is performed on an instrument equipped with 488 and 635 nm lasers. For data acquisition, the following channels are used: SSC-H, FSC-H, FL1-H (488 nm laser, 530/30 filter), FL3-H (488 nm laser, 650LP filter) and FL4-H (635 nm laser, 661/16 filter).
2. Set laser voltage (gain) and compensation unstained cells and cells stained with each fluorochrome separately.
3. If possible, acquire $>10,000$ CD38⁺ events per sample, ideally at a flow rate <500 events/s (*see Note 16*).
4. For gating (*Fig. 1*), proceed as follows:
 - a. Gate CD38⁺ cells on a SSC-H *vs.* CD38-APC (FL4-H) dot plot window (*see Note 17*).
 - b. Gate viable CD38⁺/7-AAD⁻ plasma cells on a CD38-APC (FL4-H) *vs.* 7-AAD (FL3-H) dot plot (*see Notes 18,19*).

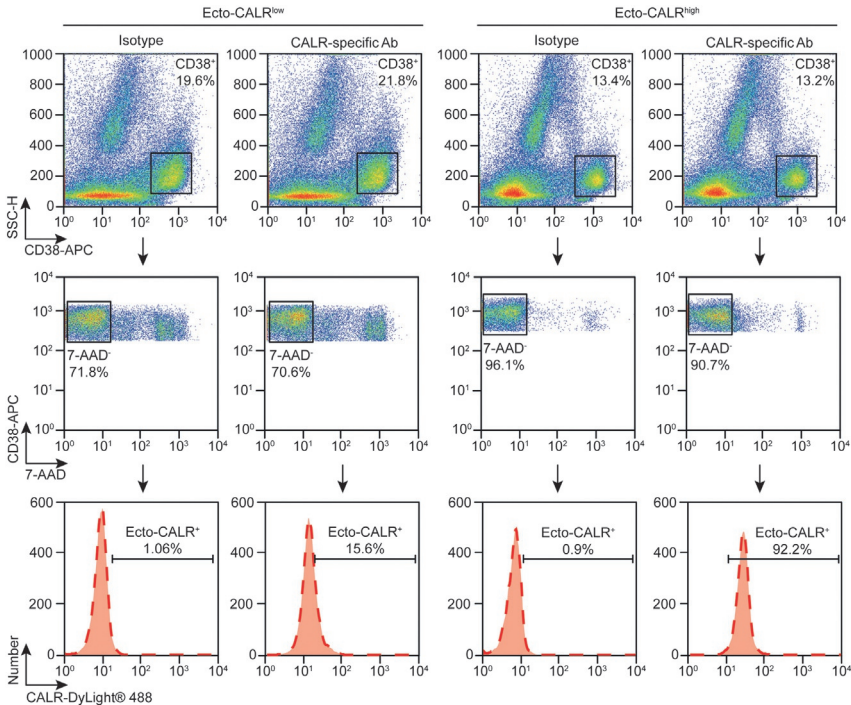


Fig. 1 Analysis of CALR exposure on live CD38⁺ plasma cells from the human bone marrow. Bone marrow mononuclear cells (BMMCs) isolated from patient-derived bone marrow samples as detailed in Section 3.1 were stained with fluorescent antibodies specific for calreticulin (CALR), or isotype controls, and CD38 in the presence of 7-AAD as a vital dye, as detailed in Section 3.2, followed by signal acquisition on flow cytometry and gating as detailed in Section 3.3. Representative dot plots and histograms from a sample with low surface-exposed CALR (Ecto-CALR^{low}) and an Ecto-CALR^{high} sample are reported. Percentages indicate the number of events within specific gates.

- c. Based on the CD38⁺/7-AAD⁻ dot plot, create a histogram for DyLight™ 488 (FL1-H). Set the gate for surface-exposed CALR positivity based on the fluorescent signal of Mouse IgG1 Isotype Control (MOPC-21), DyLight™ (<1% positivity) (*see Note 20*).

3.4 Surface-exposed PS quantification

1. Transfer 5×10^5 primary BMMCs to 5 mL Round-Bottom Polypropylene Test Tubes (*see Note 14*), and centrifuge at $335 \times g$ for 5 min.
2. Immediately resuspend BMMCs in 100 μ L in Annexin Binding Buffer (ABB) as provided in the Annexin V-DY-634 PI Apoptosis Staining/Detection Kit (*see Note 21*).

3. Add 4 μL FITC Mouse Anti-Human CD38 (HIT2), 0.5 μL Annexin V-DY-634 (1 mg/mL) and 1 μL 7-AAD Viability Staining Solution to each sample (see Note 22).
4. Incubate at RT for 15–20 min.
5. Dilute samples with 200–300 μL ABB for acquisition of fluorescent signals by flow cytometry.

3.5 Acquisition and gating

1. Flow cytometry is performed on an instrument equipped with 488 and 635 nm lasers. For data acquisition, the following channels are used: SSC, FSC, FL1-H (488 nm laser, 530/30 filter), FL3-H (488 nm laser, 650LP filter), and FL4-H (635 nm laser, 661/16 filter).
2. For gating (Fig. 2), proceeds as follow:
 - a. Gate CD38⁺ cells on a SSC-H vs. CD38-FITC (FL1-H) dot plot (see Note 17).
 - b. Gate viable CD38⁺/7-AAD⁻ plasma cells on a CD38-APC (FL4-H) vs. 7-AAD (FL3-H) dot plot (see Note 18,19).
 - c. Based on the CD38⁺/7-AAD⁻ dot plot, create a histogram for DY-634 (FL4-H). Set the gate for surface-expose PS positivity based in the closed proximity of the major peak (see Note 23).



4. Notes

1. Virtually equivalent disposable, reagents, instruments and software can be purchased from multiple other providers at a similar cost.

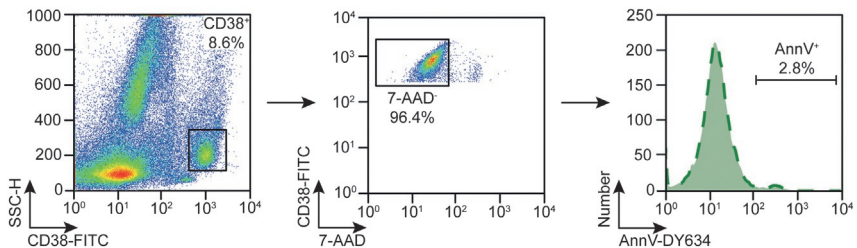


Fig. 2 Analysis of PS exposure on live CD38⁺ plasma cells from the human bone marrow. Bone marrow mononuclear cells (BMMCs) isolated from patient-derived bone marrow samples as detailed in Section 3.1 were stained with fluorescent antibodies specific for CD38 plus fluorescent Annexin V (AnnV) in the presence of 7-AAD as a vital dye, as detailed in Section 3.4, followed by signal acquisition on flow cytometry and gating as detailed in Section 3.5. Representative dot plots and histograms from one sample are reported. Percentages indicate the numbers of event within specific gates.

2. As an alternative, Annexin V can be produced, purified and conjugated with DY-634 as detailed in Ref. [Logue et al. \(2009\)](#).
3. BM samples can be obtained by hematology hospital services or biobanks. Importantly, all studies handling human samples must be conducted according to the guidelines established by the Declaration of Helsinki ([Hurst, 2014](#); [Millum et al., 2013](#); [Parsa-Parsi et al., 2013](#); [World Medical, 2013](#)). Additionally, written informed consent must be obtained from all subjects involved in the study.
4. 100 U/mL IL-6 (PeproTech, #200-06) must be added to the BMMC complete medium to carry out experiments determining the exposure of CALR or PS on the surface of CD38⁺ plasma cells as driven by experimental interventions (during which plasma cells remain in culture). However, IL-6 is dispensable for direct *ex vivo* studies (when culture is not required).
5. PBS can also be prepared according to the following recipe: 137 mM NaCl, 10 mM Na₂HPO₄, and 1.8 mM KH₂PO₄, pH: 7.4.
6. Cell counting can also be performed on a common hemocytometer such as Neubauer or a Burkler chamber.
7. The incubator is needed to quantify the exposure of CALR or PS on the surface of CD38⁺ plasma cells as driven by experimental interventions, but not for direct *ex vivo* determinations (*see also Note 4*).
8. This is important to inactivate the complement system normally contained in FBS, which may otherwise lyse BMMCs (as well as other hematopoietic cells) ([Ayuk et al., 2005](#); [Celis & Celis, 1983](#); [Zand et al., 2006](#)).
9. Volume is normally limited (2–5 mL) as the clinical procedure to obtain samples is very invasive and samples are primarily used for diagnostic procedures.
10. In the case that phases mix with each other, the experiment is compromised.
11. Electronic pipet-aids should be placed in drop-wise mode to minimize the chances of mixing phases.
12. Deactivating the brake is important to prevent separated phases to mix owing to an excessively harsh deceleration.
13. This is optional but recommended. Considerable care should be employed to avoid interfering with the BMMC layer.
14. Staining can also be performed in 1.5 mL microcentrifuge tubes but sample should next be transferred to 5 mL Round-Bottom Polypropylene Test Tubes for flow cytometry.

15. Protecting samples for direct light minimizes fluorochrome photo-bleaching, which may otherwise negatively impact on signal acquisition.
16. A reduced flow rate ensures sharper signal detection.
17. The percentage of CD38⁺ plasma cells may be useful for additional analyses and/or experiment planning. A more accurate assessment of CD38⁺ plasma cell abundance can be obtained directly staining 100 μ L of the BMMC suspension with 8 μ L APC or 4 μ L FITC Mouse Anti-Human CD38 (HIT2) followed by flow cytometry. Only samples containing >0.1% CD38⁺ plasma cells are suitable for additional experiments.
18. 7-AAD negativity is particularly important to ensure that surface-exposed (rather than total) CALR or PS is selectively detected.
19. Viability can also be conveniently assessed with propidium iodide (Miltenyi Biotec, #130-093-233), TO-PRO-3 (Invitrogen, #10710194) or DAPI (Thermo Scientific, #10116287), upon ensuring no spectral overlap with the antibody in use.
20. Mean Fluorescence Intensity (MFI) can also be employed to quantify CALR exposure upon normalization to MFI in the same sample stained with isotype control antibodies.
21. This is important as the binding between PS and Annexin V is Ca²⁺-dependent (Blackwood & Ernst, 1990; Lemmon, 2008; Schlaepfer et al., 1987). If recombinant Annexin V is produced and conjugated with DY-634 in the laboratory, an adequate ABB can be obtained as per the following recipe: 10 mM HEPES/NaOH, 140 mM NaCl and 2.5 mM CaCl₂ in PBS, pH: 7.4.
22. While these volumes refer to a single sample, the staining solution should be prepared collectively for all samples included in the experiments (including 10% surplus) to homogenize staining conditions.
23. MFI is generally not employed to quantify PS exposure.



5. Concluding remarks

Stressed and dying cells expose a number of molecules on their surface, and this is paramount for the organism to properly react to cell death in support of systemic homeostasis (Freeman & Grinstein, 2021; Galluzzi et al., 2018; Poon & Ravichandran, 2024). In this context, CALR and PS mediate diametrically opposed functions, the former promoting phagocytosis by APC precursors, which potentially culminates with adaptive immune responses, the latter promoting efferocytosis by macrophages,

which generally results in suppressed inflammation and immunity (Boada-Romero et al., 2020; Mehrotra & Ravichandran, 2022; Rothlin et al., 2021). Thus, assessing the propensity of malignant cells to spontaneously expose CALR or PS on their surface may not only provide insights into the overall degree of stress these cells are experiencing *in vivo*, but also convey prognostic and/or predictive information, as previously demonstrated in a number of patient cohorts (Fucikova et al., 2015). Along similar lines, testing the propensity of malignant cells to expose CALR or PS on their surface upon therapy (be it *in vivo* or *ex vivo*) may provide valuable information for the design of novel therapeutic strategies building on the induction of ICD (Bezu et al., 2015; Calvillo-Rodríguez et al., 2023; Ghiringhelli & Rébé, 2024; Mishchenko et al., 2024; Pan et al., 2024; Vacchelli et al., 2012).

The protocol detailed herein provides a simple method to specifically quantify CALR and PS levels on the surface of viable CD38⁺ plasma cells by flow cytometry, which (with some variations reflecting tissue of origin and species) should be simply adaptable to other malignant cells from humans and rodents. To obtain an increasingly precise characterization of intratumoral heterogeneity in MM with respect to CALR and PS exposure, we ultimately aim at introducing key immunophenotypic MM markers in this analysis, notably, CD19, syndecan 1 (SDC1, best known as CD138), protein tyrosine phosphatase receptor type C (PTPRC, best known as CD45), neural cell adhesion molecule 1 (NCAM1, best known as CD56) and KIT proto-oncogene, receptor tyrosine kinase (KIT, also known as CD117 (Kumar et al., 2010; San Miguel et al., 2002). Despite these and other possible ameliorations, the flow cytometry-assisted quantification of CALR and PS on CD38⁺ plasma cells stands out as a convenient tool to investigate spontaneous or therapy-driven immunogenic stress responses in BM samples from patients with MM.

Acknowledgments

M.B.-V. was supported by a predoctoral fellowship from Spanish Ministry of Universities (FPU17/02586) and A.S.-D.V. and N.J.-A. were also supported by a predoctoral fellowship from Gobierno de Aragón. The L.G. lab is/has been supported (as a PI unless otherwise indicated) by one NIH R01 grant (#CA271915), by two Breakthrough Level 2 grants from the US DoD BCRP (#BC180476P1, #BC210945), by a grant from the STARR Cancer Consortium (#I16-0064), by a Transformative Breast Cancer Consortium Grant from the US DoD BCRP (#W81XWH2120034, PI: Formenti), by a U54 grant from NIH/NCI (#CA274291, PI: Deasy, Formenti, Weichselbaum), by the 2019 Laura Ziskin Prize in Translational Research (#ZP-6177, PI: Formenti) from the

Stand Up to Cancer (SU2C), by a Mantle Cell Lymphoma Research Initiative (MCL-RI, PI: Chen-Kiang) grant from the Leukemia and Lymphoma Society (LLS), by a Rapid Response Grant from the Functional Genomics Initiative (New York, US), by a pre-SPORE grant (PI: Demaria, Formenti), a Collaborative Research Initiative Grant and a Clinical Trials Innovation Grant from the Sandra and Edward Meyer Cancer Center (New York, US), by startup funds from the Dept. of Radiation Oncology at Weill Cornell Medicine (New York, US), by industrial collaborations with Lytix Biopharma (Oslo, Norway), Promontory (New York, US) and Onxeo (Paris, France), as well as by donations from Promontory (New York, US), the Luke Heller TECPR2 Foundation (Boston, US), Sotio a.s. (Prague, Czech Republic), Lytix Biopharma (Oslo, Norway), Onxeo (Paris, France), Ricerchiamo (Brescia, Italy), and Noxopharm (Chatswood, Australia). The IM lab is/has been supported by grants #PID2019-105128RB-I00 and #PID2022-136799OB-I00 funded by MCIN/AEI/10.13039/501100011033 and grant #B31_20R funded by Gobierno de Aragón.

Conflicts of interests

L.G. is/has been holding research contracts with Lytix Biopharma, Promontory and Onxeo, has received consulting/advisory honoraria from Boehringer Ingelheim, AstraZeneca, AbbVie, OmniSEQ, Onxeo, The Longevity Labs, Inzen, Invax, Sotio, Promontory, Noxopharm, EduCom, and the Luke Heller TECPR2 Foundation, and holds Promontory stock options. The other authors have no conflicts of interest to declare.

References

- Adkins, I., et al. (2014). Physical modalities inducing immunogenic tumor cell death for cancer immunotherapy. *Oncoimmunology*, 3, e968434. <https://doi.org/10.4161/21624011.2014.968434>.
- Ayuk, F. A., et al. (2005). Antithymocyte globulin induces complement-dependent cell lysis and caspase-dependent apoptosis in myeloma cells. *Experimental Hematology*, 33, 1531–1536. <https://doi.org/10.1016/j.exphem.2005.08.004>.
- Bezu, L., et al. (2015). Combinatorial strategies for the induction of immunogenic cell death. *Frontiers in Immunology*, 6, 187. <https://doi.org/10.3389/fimmu.2015.00187>.
- Bezu, L., et al. (2018a). eIF2 α phosphorylation: A hallmark of immunogenic cell death. *Oncoimmunology*, 7, e1431089. <https://doi.org/10.1080/2162402x.2018.1431089>.
- Bezu, L., et al. (2018b). eIF2 α phosphorylation is pathognomonic for immunogenic cell death. *Cell Death and Differentiation*, 25, 1375–1393. <https://doi.org/10.1038/s41418-017-0044-9>.
- Blackwood, R. A., & Ernst, J. D. (1990). Characterization of Ca²⁺(+)-dependent phospholipid binding, vesicle aggregation and membrane fusion by annexins. *The Biochemical Journal*, 266, 195–200. <https://doi.org/10.1042/bj2660195>.
- Boada-Romero, E., et al. (2020). The clearance of dead cells by efferocytosis. *Nature Reviews. Molecular Cell Biology*, 21, 398–414. <https://doi.org/10.1038/s41580-020-0232-1>.
- Böttcher, J. P., et al. (2018). NK cells stimulate recruitment of cDC1 into the tumor microenvironment promoting cancer immune control. *Cell*, 172, 1022–1037. e1014. <https://doi.org/10.1016/j.cell.2018.01.004>.
- Calvillo-Rodríguez, K. M., et al. (2023). Immunotherapies inducing immunogenic cell death in cancer: Insight of the innate immune system. *Frontiers in Immunology*, 14, 1294434. <https://doi.org/10.3389/fimmu.2023.1294434>.
- Casares, N., et al. (2005). Caspase-dependent immunogenicity of doxorubicin-induced tumor cell death. *The Journal of Experimental Medicine*, 202, 1691–1701. <https://doi.org/10.1084/jem.20050915>.

- Celis, B., & Celis, E. (1983). Complement-mediated killing of myeloma tumour cells: Differences in susceptibility to lysis by antibodies and complement are independent of antigen expression and antibody binding. *Immunology*, *49*, 321–328.
- Cytlak, U. M., et al. (2022). Immunomodulation by radiotherapy in tumour control and normal tissue toxicity. *Nature Reviews. Immunology*, *22*, 124–138. <https://doi.org/10.1038/s41577-021-00568-1>.
- Czabotar, P. E., & Garcia-Saez, A. J. (2023). Mechanisms of BCL-2 family proteins in mitochondrial apoptosis. *Nature Reviews. Molecular Cell Biology*, *24*, 732–748. <https://doi.org/10.1038/s41580-023-00629-4>.
- Diepstraten, S. T., et al. (2022). The manipulation of apoptosis for cancer therapy using BH3-mimetic drugs. *Nature Reviews. Cancer*, *22*, 45–64. <https://doi.org/10.1038/s41568-021-00407-4>.
- Doran, A. C., et al. (2020). Efferocytosis in health and disease. *Nature Reviews. Immunology*, *20*, 254–267. <https://doi.org/10.1038/s41577-019-0240-6>.
- Efimova, I., et al. (2020). Vaccination with early ferroptotic cancer cells induces efficient antitumor immunity. *Journal for Immunotherapy of Cancer*, *8*. <https://doi.org/10.1136/jitc-2020-001369>.
- Fadok, V. A., et al. (1992). Exposure of phosphatidylserine on the surface of apoptotic lymphocytes triggers specific recognition and removal by macrophages. *Journal of Immunology*, *148*, 2207–2216.
- Fadok, V. A., et al. (2000). A receptor for phosphatidylserine-specific clearance of apoptotic cells. *Nature*, *405*, 85–90. <https://doi.org/10.1038/35011084>.
- Freeman, S., & Grinstein, S. (2021). Promoters and antagonists of phagocytosis: A plastic and tunable response. *Annual Review of Cell and Developmental Biology*, *37*, 89–114. <https://doi.org/10.1146/annurev-cellbio-120219-055903>.
- Fuchs, Y., & Steller, H. (2015). Live to die another way: Modes of programmed cell death and the signals emanating from dying cells. *Nature Reviews. Molecular Cell Biology*, *16*, 329–344. <https://doi.org/10.1038/nrm3999>.
- Fucikova, J., et al. (2015). Prognostic and predictive value of DAMPs and DAMP-associated processes in Cancer. *Frontiers in Immunology*, *6*, 402. <https://doi.org/10.3389/fimmu.2015.00402>.
- Fucikova, J., et al. (2016a). Calreticulin expression in human non-small cell lung cancers correlates with increased accumulation of antitumor immune cells and favorable prognosis. *Cancer Research*, *76*, 1746–1756. <https://doi.org/10.1158/0008-5472.Can-15-1142>.
- Fucikova, J., et al. (2016b). Calreticulin exposure by malignant blasts correlates with robust anticancer immunity and improved clinical outcome in AML patients. *Blood*, *128*, 3113–3124. <https://doi.org/10.1182/blood-2016-08-731737>.
- Fucikova, J., et al. (2021). Calreticulin and cancer. *Cell Research*, *31*, 5–16. <https://doi.org/10.1038/s41422-020-0383-9>.
- Galluzzi, L., et al. (2018). Linking cellular stress responses to systemic homeostasis. *Nature Reviews. Molecular Cell Biology*, *19*, 731–745. <https://doi.org/10.1038/s41580-018-0068-0>.
- Galluzzi, L., et al. (2020a). Consensus guidelines for the definition, detection and interpretation of immunogenic cell death. *Journal for Immunotherapy of Cancer*, *8*. <https://doi.org/10.1136/jitc-2019-000337>.
- Galluzzi, L., et al. (2020b). Immunostimulation with chemotherapy in the era of immune checkpoint inhibitors. *Nature Reviews. Clinical Oncology*, *17*, 725–741. <https://doi.org/10.1038/s41571-020-0413-z>.
- Galluzzi, L., et al. (2023). Immunogenic cell death in cancer: Concept and therapeutic implications. *Journal of Translational Medicine*, *21*, 162. <https://doi.org/10.1186/s12967-023-04017-6>.

- Gardai, S. J., et al. (2005). Cell-surface calreticulin initiates clearance of viable or apoptotic cells through trans-activation of LRP on the phagocyte. *Cell*, 123, 321–334. <https://doi.org/10.1016/j.cell.2005.08.032>.
- Garg, A. D., et al. (2016). Dendritic cell vaccines based on immunogenic cell death elicit danger signals and T cell-driven rejection of high-grade glioma. *Science Translational Medicine*, 8. <https://doi.org/10.1126/scitranslmed.aae01105>. 328ra327.
- Ghiringhelli, F., & Rébé, C. (2024). Using immunogenic cell death to improve anticancer efficacy of immune checkpoint inhibitors: From basic science to clinical application. *Immunological Reviews*, 321, 335–349. <https://doi.org/10.1111/immr.13263>.
- Giampazolias, E., et al. (2017). Mitochondrial permeabilization engages NF- κ B-dependent anti-tumour activity under caspase deficiency. *Nature Cell Biology*, 19, 1116–1129. <https://doi.org/10.1038/ncb3596>.
- Gong, T., et al. (2020). DAMP-sensing receptors in sterile inflammation and inflammatory diseases. *Nature Reviews. Immunology*, 20, 95–112. <https://doi.org/10.1038/s41577-019-0215-7>.
- Hadian, K., & Stockwell, B. R. (2023). The therapeutic potential of targeting regulated non-apoptotic cell death. *Nature Reviews. Drug Discovery*, 22, 723–742. <https://doi.org/10.1038/s41573-023-00749-8>.
- Han, C., et al. (2020). Tumor cells suppress radiation-induced immunity by hijacking caspase 9 signaling. *Nature Immunology*, 21, 546–554. <https://doi.org/10.1038/s41590-020-0641-5>.
- Harrington, K., et al. (2019). Optimizing oncolytic virotherapy in cancer treatment. *Nature Reviews. Drug Discovery*, 18, 689–706. <https://doi.org/10.1038/s41573-019-0029-0>.
- Hsu, W. M., et al. (2005). Calreticulin expression in neuroblastoma—A novel independent prognostic factor. *Annals of Oncology*, 16, 314–321. <https://doi.org/10.1093/annonc/mdi062>.
- Huang, Q., et al. (2011). Caspase 3-mediated stimulation of tumor cell repopulation during cancer radiotherapy. *Nature Medicine*, 17, 860–866. <https://doi.org/10.1038/nm.2385>.
- Hurst, S. A. (2014). Declaration of Helsinki and protection for vulnerable research participants. *JAMA*, 311, 1252. <https://doi.org/10.1001/jama.2014.1272>.
- Jhunjhunwala, S., et al. (2021). Antigen presentation in cancer: Insights into tumour immunogenicity and immune evasion. *Nature Reviews. Cancer*, 21, 298–312. <https://doi.org/10.1038/s41568-021-00339-z>.
- Kasikova, L., et al. (2019). Calreticulin exposure correlates with robust adaptive antitumor immunity and favorable prognosis in ovarian carcinoma patients. *Journal for Immunotherapy of Cancer*, 7, 312. <https://doi.org/10.1186/s40425-019-0781-z>.
- Kepp, O., et al. (2020). Oncolysis without viruses—Inducing systemic anticancer immune responses with local therapies. *Nature Reviews. Clinical Oncology*, 17, 49–64. <https://doi.org/10.1038/s41571-019-0272-7>.
- Kroemer, G., et al. (2022). Immunogenic cell stress and death. *Nature Immunology*, 23, 487–500. <https://doi.org/10.1038/s41590-022-01132-2>.
- Krysko, D. V., et al. (2012). Immunogenic cell death and DAMPs in cancer therapy. *Nature Reviews. Cancer*, 12, 860–875. <https://doi.org/10.1038/nrc3380>.
- Kumar, S., et al. (2010). Immunophenotyping in multiple myeloma and related plasma cell disorders. *Best Practice & Research. Clinical Haematology*, 23, 433–451. <https://doi.org/10.1016/j.beha.2010.09.002>.
- Lang, F., et al. (2022). Identification of neoantigens for individualized therapeutic cancer vaccines. *Nature Reviews. Drug Discovery*, 21, 261–282. <https://doi.org/10.1038/s41573-021-00387-y>.
- Lei, G., et al. (2022). Targeting ferroptosis as a vulnerability in cancer. *Nature Reviews. Cancer*, 22, 381–396. <https://doi.org/10.1038/s41568-022-00459-0>.
- Lemmon, M. A. (2008). Membrane recognition by phospholipid-binding domains. *Nature Reviews. Molecular Cell Biology*, 9, 99–111. <https://doi.org/10.1038/nrm2328>.

- Li, M. O., et al. (2003). Phosphatidylserine receptor is required for clearance of apoptotic cells. *Science*, 302, 1560–1563. <https://doi.org/10.1126/science.1087621>.
- Logue, S. E., et al. (2009). Expression, purification and use of recombinant annexin V for the detection of apoptotic cells. *Nature Protocols*, 4, 1383–1395. <https://doi.org/10.1038/nprot.2009.143>.
- Matzinger, P. (2002). The danger model: A renewed sense of self. *Science*, 296, 301–305. <https://doi.org/10.1126/science.1071059>.
- McLaughlin, M., et al. (2020). Inflammatory microenvironment remodelling by tumour cells after radiotherapy. *Nature Reviews. Cancer*, 20, 203–217. <https://doi.org/10.1038/s41568-020-0246-1>.
- Mehrotra, P., & Ravichandran, K. S. (2022). Drugging the efferocytosis process: Concepts and opportunities. *Nature Reviews. Drug Discovery*, 21, 601–620. <https://doi.org/10.1038/s41573-022-00470-y>.
- Mellman, I., et al. (2023). The cancer-immunity cycle: Indication, genotype, and immunotype. *Immunity*, 56, 2188–2205. <https://doi.org/10.1016/j.immuni.2023.09.011>.
- Millum, J., et al. (2013). The 50th anniversary of the declaration of Helsinki: Progress but many remaining challenges. *JAMA*, 310, 2143–2144. <https://doi.org/10.1001/jama.2013.281632>.
- Mishchenko, T. A., et al. (2024). Targeting immunogenic cell death for glioma immunotherapy. *Trends in Cancer*, 10, 8–11. <https://doi.org/10.1016/j.trecan.2023.10.005>.
- Ning, X., et al. (2019). Apoptotic caspases suppress type I interferon production via the cleavage of cGAS, MAVS, and IRF3. *Molecular Cell*, 74, 19–31. e17 <https://doi.org/10.1016/j.molcel.2019.02.013>.
- Obeid, M., et al. (2007). Leveraging the immune system during chemotherapy: Moving calreticulin to the cell surface converts apoptotic death from “silent” to immunogenic. *Cancer Research*, 67, 7941–7944. <https://doi.org/10.1158/0008-5472.Can-07-1622>.
- Ogden, C. A., et al. (2001). C1q and mannose binding lectin engagement of cell surface calreticulin and CD91 initiates macropinocytosis and uptake of apoptotic cells. *The Journal of Experimental Medicine*, 194, 781–795. <https://doi.org/10.1084/jem.194.6.781>.
- Palanivelu, L., et al. (2022). Immunogenic cell death: The cornerstone of oncolytic viro-immunotherapy. *Frontiers in Immunology*, 13, 1038226. <https://doi.org/10.3389/fimmu.2022.1038226>.
- Pan, H., et al. (2024). Preconditioning with immunogenic cell death-inducing treatments for subsequent immunotherapy. *International Review of Cell and Molecular Biology*, 382, 279–294. <https://doi.org/10.1016/bs.ircmb.2023.06.001>.
- Panaretakis, T., et al. (2009). Mechanisms of pre-apoptotic calreticulin exposure in immunogenic cell death. *The EMBO Journal*, 28, 578–590. <https://doi.org/10.1038/emboj.2009.1>.
- Parsa-Parsi, R., et al. (2013). Reconsidering the declaration of Helsinki. *Lancet*, 382, 1246–1247. [https://doi.org/10.1016/S0140-6736\(13\)62094-2](https://doi.org/10.1016/S0140-6736(13)62094-2).
- Pawaria, S., & Binder, R. J. (2011). CD91-dependent programming of T-helper cell responses following heat shock protein immunization. *Nature Communications*, 2, 521. <https://doi.org/10.1038/ncomms1524>.
- Peng, R. Q., et al. (2010). Expression of calreticulin is associated with infiltration of T-cells in stage IIIB colon cancer. *World Journal of Gastroenterology*, 16, 2428–2434. <https://doi.org/10.3748/wjg.v16.i19.2428>.
- Poon, I. K. H., & Ravichandran, K. S. (2024). Targeting efferocytosis in inflammaging. *Annual Review of Pharmacology and Toxicology*, 64, 339–357. <https://doi.org/10.1146/annurev-pharmtox-032723-110507>.
- Rodriguez-Ruiz, M. E., et al. (2019). Apoptotic caspases inhibit abscopal responses to radiation and identify a new prognostic biomarker for breast cancer patients. *Oncimmunology*, 8, e1655964. <https://doi.org/10.1080/2162402x.2019.1655964>.

- Rodriguez-Ruiz, M. E., et al. (2020). Immunological impact of cell death signaling driven by radiation on the tumor microenvironment. *Nature Immunology*, *21*, 120–134. <https://doi.org/10.1038/s41590-019-0561-4>.
- Rongvaux, A., et al. (2014). Apoptotic caspases prevent the induction of type I interferons by mitochondrial DNA. *Cell*, *159*, 1563–1577. <https://doi.org/10.1016/j.cell.2014.11.037>.
- Rothlin, C. V., et al. (2021). Determining the effector response to cell death. *Nature Reviews. Immunology*, *21*, 292–304. <https://doi.org/10.1038/s41577-020-00456-0>.
- San Miguel, J. F., et al. (2002). Immunophenotypic evaluation of the plasma cell compartment in multiple myeloma: A tool for comparing the efficacy of different treatment strategies and predicting outcome. *Blood*, *99*, 1853–1856. <https://doi.org/10.1182/blood.v99.5.1853>.
- Schlaepfer, D. D., et al. (1987). Structural and functional characterization of endonexin II, a calcium- and phospholipid-binding protein. *Proceedings of the National Academy of Sciences of the United States of America*, *84*, 6078–6082. <https://doi.org/10.1073/pnas.84.17.6078>.
- Serrano Del Valle, A., et al. (2022). Ecto-calreticulin expression in multiple myeloma correlates with a failed anti-tumoral immune response and bad prognosis. *Oncoimmunology*, *11*, 2141973. <https://doi.org/10.1080/2162402x.2022.2141973>.
- Shalhout, S. Z., et al. (2023). Therapy with oncolytic viruses: Progress and challenges. *Nature Reviews. Clinical Oncology*, *20*, 160–177. <https://doi.org/10.1038/s41571-022-00719-w>.
- Sprooten, J., et al. (2023). Trial watch: Chemotherapy-induced immunogenic cell death in oncology. *Oncoimmunology*, *12*, 2219591. <https://doi.org/10.1080/2162402x.2023.2219591>.
- Stern, L. J., et al. (2024). Non-mutational neoantigens in disease. *Nature Immunology*, *25*, 29–40. <https://doi.org/10.1038/s41590-023-01664-1>.
- Tatsuno, K., et al. (2019). Extracorporeal photochemotherapy induces bona fide immunogenic cell death. *Cell Death & Disease*, *10*, 578. <https://doi.org/10.1038/s41419-019-1819-3>.
- Truxova, I., et al. (2020). Calreticulin exposure on malignant blasts correlates with improved natural killer cell-mediated cytotoxicity in acute myeloid leukemia patients. *Haematologica*, *105*, 1868–1878. <https://doi.org/10.3324/haematol.2019.223933>.
- Vacchelli, E., et al. (2012). Trial watch: Chemotherapy with immunogenic cell death inducers. *Oncoimmunology*, *1*, 179–188. <https://doi.org/10.4161/onci.1.2.19026>.
- Vandivier, R. W., et al. (2002). Role of surfactant proteins a, D, and C1q in the clearance of apoptotic cells in vivo and in vitro: Calreticulin and CD91 as a common collectin receptor complex. *Journal of Immunology*, *169*, 3978–3986. <https://doi.org/10.4049/jimmunol.169.7.3978>.
- Ventura, A., et al. (2018). Extracorporeal photochemotherapy drives monocyte-to-dendritic cell maturation to induce anticancer immunity. *Cancer Research*, *78*, 4045–4058. <https://doi.org/10.1158/0008-5472.Can-18-0171>.
- Vitale, I., et al. (2023). Apoptotic cell death in disease—Current understanding of the NCCD 2023. *Cell Death and Differentiation*, *30*, 1097–1154. <https://doi.org/10.1038/s41418-023-01153-w>.
- Wemeau, M., et al. (2010). Calreticulin exposure on malignant blasts predicts a cellular anticancer immune response in patients with acute myeloid leukemia. *Cell Death & Disease*, *1*, e104. <https://doi.org/10.1038/cddis.2010.82>.
- White, M. J., et al. (2014). Apoptotic caspases suppress mtDNA-induced STING-mediated type I IFN production. *Cell*, *159*, 1549–1562. <https://doi.org/10.1016/j.cell.2014.11.036>.
- World Medical A. (2013). World medical association declaration of Helsinki: Ethical principles for medical research involving human subjects. *JAMA*, *310*, 2191–2194. <https://doi.org/10.1001/jama.2013.281053>.

- Xu, Q., et al. (2018). Significance of calreticulin as a prognostic factor in endometrial cancer. *Oncology Letters*, *15*, 8999–9008. <https://doi.org/10.3892/ol.2018.8495>.
- Yamazaki, T., et al. (2020). Mitochondrial DNA drives abscopal responses to radiation that are inhibited by autophagy. *Nature Immunology*, *21*, 1160–1171. <https://doi.org/10.1038/s41590-020-0751-0>.
- Yatim, N., et al. (2015). RIPK1 and NF- κ B signaling in dying cells determines cross-priming of CD8⁺ T cells. *Science*, *350*, 328–334. <https://doi.org/10.1126/science.aad0395>.
- Yuan, J., & Ofengeim, D. (2023). A guide to cell death pathways. *Nature Reviews. Molecular Cell Biology*. <https://doi.org/10.1038/s41580-023-00689-6>.
- Zand, M. S., et al. (2006). Apoptosis and complement-mediated lysis of myeloma cells by polyclonal rabbit antithymocyte globulin. *Blood*, *107*, 2895–2903. <https://doi.org/10.1182/blood-2005-06-2269>.
- Zelenay, S., et al. (2015). Cyclooxygenase-dependent tumor growth through evasion of immunity. *Cell*, *162*, 1257–1270. <https://doi.org/10.1016/j.cell.2015.08.015>.